

Available online at www.sciencedirect.com**ScienceDirect**

Progress in Natural Science: Materials International 24 (2014) 305–312

**Progress in Natural
Science
Materials International**www.elsevier.com/locate/pnsmi
www.sciencedirect.com

Original Research

Solid solution or amorphous phase formation in TiZr-based ternary to quinary multi-principal-element films

Mariana Braic, Viorel Braic, Alina Vladescu, Catalin N. Zoita, Mihai Balaceanu*

National Institute for Optoelectronics, 409 Atomistilor Street, PO BOX MG 05, RO77125 Magurele-Bucharest, Romania

Received 22 August 2013; accepted 20 April 2014

Available online 24 July 2014

Abstract

TiZr-based multicomponent metallic films composed of 3–5 constituents with almost equal atomic concentrations were prepared by co-sputtering of pure metallic targets in an Ar atmosphere. X-ray diffraction was employed to determine phase composition, crystalline structure, lattice parameters, texture and crystallite size of the deposited films.

The deposited films exhibited only solid solution (fcc, bcc or hcp) or amorphous phases, no intermetallic components being detected. It was found that the hcp structure was stabilized by the presence of Hf or Y, bcc by Nb or Al and fcc by Cu. For the investigated films, the atomic size difference, mixing enthalpy, mixing entropy, Gibbs free energy of mixing and the electronegativity difference for solid solution and amorphous phases were calculated based on Miedema's approach of the regular solution model. It was shown that the atomic size difference and the ratio between the Gibbs free energies of mixing of the solid solution and amorphous phases were the most significant parameters controlling the film crystallinity.

© 2014 Chinese Materials Research Society. Production and hosting by Elsevier B.V. All rights reserved.

Keywords: Multicomponent metallic films; Magnetron sputtering; X-ray diffraction; TiZr-based high-entropy alloys

1. Introduction

Multicomponent alloy systems comprising more than three elements with various atomic concentrations were found to possess complex microstructures including solid solution, amorphous phases, and/or intermetallic compounds [1–5]. Since the stability and the mechanical, tribological, anticorrosive and other characteristics of these materials are directly affected by their phase compositions and structures, it is important to predict and control the phases and the corresponding structures, by properly selecting the constituents. For example, the systems containing intermetallic compounds, in spite of their high strength and thermal resistance, are brittle, rendering their

application rather limited. Among multicomponent alloys, those commonly named high-entropy alloys (HEAs) are of special interest [6–23]. By definition [6], high-entropy alloys belong to a class of alloys composed of at least five principal metallic elements (5–13) in near-equiatomic ratios. The HEA alloys investigated so far were found to exhibit remarkable properties such as very fine structures with nanoscale precipitates and also amorphous phases, high thermal stability, superior resistance to wear, corrosion and oxidation etc., resulting from the combined effects of high Gibbs free energy of mixing (mixing entropy), lattice distortion, low long-range diffusion and “cocktail effect” [7]. The high value of the mixing entropy enhances the mutual solubility among elements leading to preferential formation of solid solutions instead of intermetallics, the lattice distortion causes solid solution hardening, the reduced diffusion promotes the formation of nanocrystalline or amorphous phases, and the “cocktail effect” exploits the merits of one or another constituent. A number of empirical rules based on the thermodynamical criteria have been developed to predict the phase formation

*Corresponding author. Tel./fax: +40 21 457 57 59.

E-mail addresses: mariana_braic@inoe.ro (M. Braic),
vbraic@inoe.ro (V. Braic), alinava@inoe.ro (A. Vladescu),
cnzoita@inoe.ro (C. N. Zoita), balaceanu@inoe.ro (M. Balaceanu).

Peer review under responsibility of Chinese Materials Research Society.

(solid solutions, intermetallic compounds and amorphous metallic glasses) for multicomponent alloys, including HEAs [14,15,18–20,24]. For instance, Zhang et al. [18], Yang and Zhang [20], and Guo et al. [14,15] extended the solid-solution-formation rules for binary systems (Hume-Rothery rules [25]) to the case of high-entropy alloys.

Beside the analysis of phase formation in bulk multicomponent alloys, a similar study in the case of multicomponent metallic thin films, including those composed of metals with equal atomic percentage (multi-principal-element or MPE films) [26–30], would be also of great interest. For example, properties improvement has been found for films containing multiple phases [31]. In the case of MPE films with 3–8 components, the various microstructures, which mainly depend on the types of constituents, significantly influence film characteristics, as thermal stability, morphology, hardness, corrosion resistance, etc. [26].

The purpose of the present study was to find out the factors controlling phase formation in TiZr-based MPE metallic films comprising 3–5 constituents, produced by co-deposition from multiple single-element targets. The TiZr-system was selected as a binary base system because the two transition metals are completely miscible in the solid state, so it forms a solid solution with structure and characteristics well known at present (e.g. [32]).

Cu, Al, Cr, Nb, Hf, Y and Si in various combinations, were specifically chosen to be added to Ti–Zr to form ternary to quinary films, because they possess different crystalline structures (fcc, bcc or hcp), mixing enthalpies and atomic radii, and this allows to examine the role of these factors in the phase formation process. Ternary TiZrHf, TiZrNb, TiZrCu and TiZrSi, quaternary TiZrHfNb, TiZrHfY, TiZrHfCu and TiZrCuSi, and quinary TiZrHfNbAl, TiZrHfNbCr, TiZrHfNbY, TiZrHfNbCu and TiZrCuYSi films were prepared and investigated. For comparison, binary TiZr films were also examined.

Film characterization was performed in terms of elemental and phase composition, texture, crystalline structure and crystallite size. Since the film crystallinity was appreciated by X-ray diffraction, the investigated films could be termed as XRD crystalline or XRD amorphous films. A possible formation of minor ordered phases in the amorphous films, observable by HRTEM examination, was not considered in this work. In the following the films will be named either crystalline or amorphous, the denotation “solid solution” implying a crystalline structure.

2. Material and methods

The films were deposited on D3 tool steel substrates by co-sputtering of two to five metallic targets made of Ti, Zr, Hf, Cu, Cr, Al, Nb, Y or Si, in Ar atmosphere, using an ATC ORION magnetron sputtering unit (AJA Int.). Prior to deposition, the samples were sputter cleaned with Ar⁺ (1000 eV, 10 min). The deposition chamber was pumped down to $\sim 2 \times 10^{-5}$ Pa. By preliminary experiments, the power applied to each target was adjusted for obtaining films with near-equiatom concentrations of the composing elements.

The main deposition parameters were: Ar flow rate = 10 sccm; power fed to targets ~ 250 W (Ti), ~ 140 W (Zr), ~ 210 W (Hf), ~ 200 W (Cu), ~ 125 W (Cr), ~ 150 W (Al), ~ 100 W (Nb), ~ 120 W (Y), and ~ 300 W (Si); substrate bias voltage = -100 V; deposition temperature = 300 °C; deposition duration = 110–130 min, in order to obtain films with constant thickness (~ 2.8 μm). For TiZr film preparation, two cathodes of each type (Ti and Zr) were used in order to have similar deposition rates and ion bombardment conditions as for the MPE films.

The elemental compositions of the films were determined by energy dispersive X-ray spectroscopy (EDS) using an electron probe micro-analyzer (XL-30-ESEM TMO) equipped with energy dispersive X-ray spectrometer. X-ray diffraction analysis (Rigaku MiniFlex II, with Cu K α radiation) was carried out to investigate the phase composition, crystalline structure, lattice parameters and crystallite size of the deposited films.

3. Results

The determination of the atomic concentrations of the elements, as derived from quantitative EDS analysis, showed that for a certain coating type the atomic concentrations of the components were similar, within $\pm 7\%$ accuracy. Therefore, for calculating the thermodynamic functions controlling the phase formation, in the following, the atomic concentrations of different elements in a certain film type will be considered as being equal.

The XRD patterns of the deposited films are presented in Fig. 1. Lattice parameters and crystallite sizes (estimated from the Scherrer formula), as derived from XRD spectra, are listed in Table 1. The experimental results showed that the deposited films did not exhibit the formation of intermetallic compounds. On the other side, as seen in Fig. 1 and Table 1, the crystalline structure, film crystallinity and crystallite size were strongly sensitive to the type and number of film constituents. For the crystalline films, crystallite sizes in the range 2–25 nm were calculated.

The binary Ti–Zr system exhibited, in line with the existing data (reference JLPDS card 03-065-9625), a hexagonal (hcp-type) crystalline structure, with lattice parameters $a = 0.3111$ nm and $c = 0.4887$ nm (crystallite size $\langle d \rangle = 14.2$ nm).

For the ternary compounds (TiZrHf, TiZrNb, TiZrY, TiZrCu and TiZrSi), the addition of different elements to TiZr affected the crystalline structure in different ways. The addition of Hf (hcp structure) maintained the hcp structure of the compound (TiZrHf), whereas Nb (bcc) led to bcc structure of TiZrNb. As for the crystallinity, the TiZrHf and TiZrNb films were crystalline, TiZrCu and TiZrSi and TiZrY were amorphous, despite the different crystalline structures of the added elements.

For the quaternary films containing three elements with hcp structure, the incorporation of Nb (bcc structure) promoted a bcc phase, while the Y (hcp) addition led to the formation of a mixture of two distinct hcp phases. As expected from the observed structure of the ternary films containing Cu and Si, the TiZrHfCu and TiZrSiCu films were amorphous.

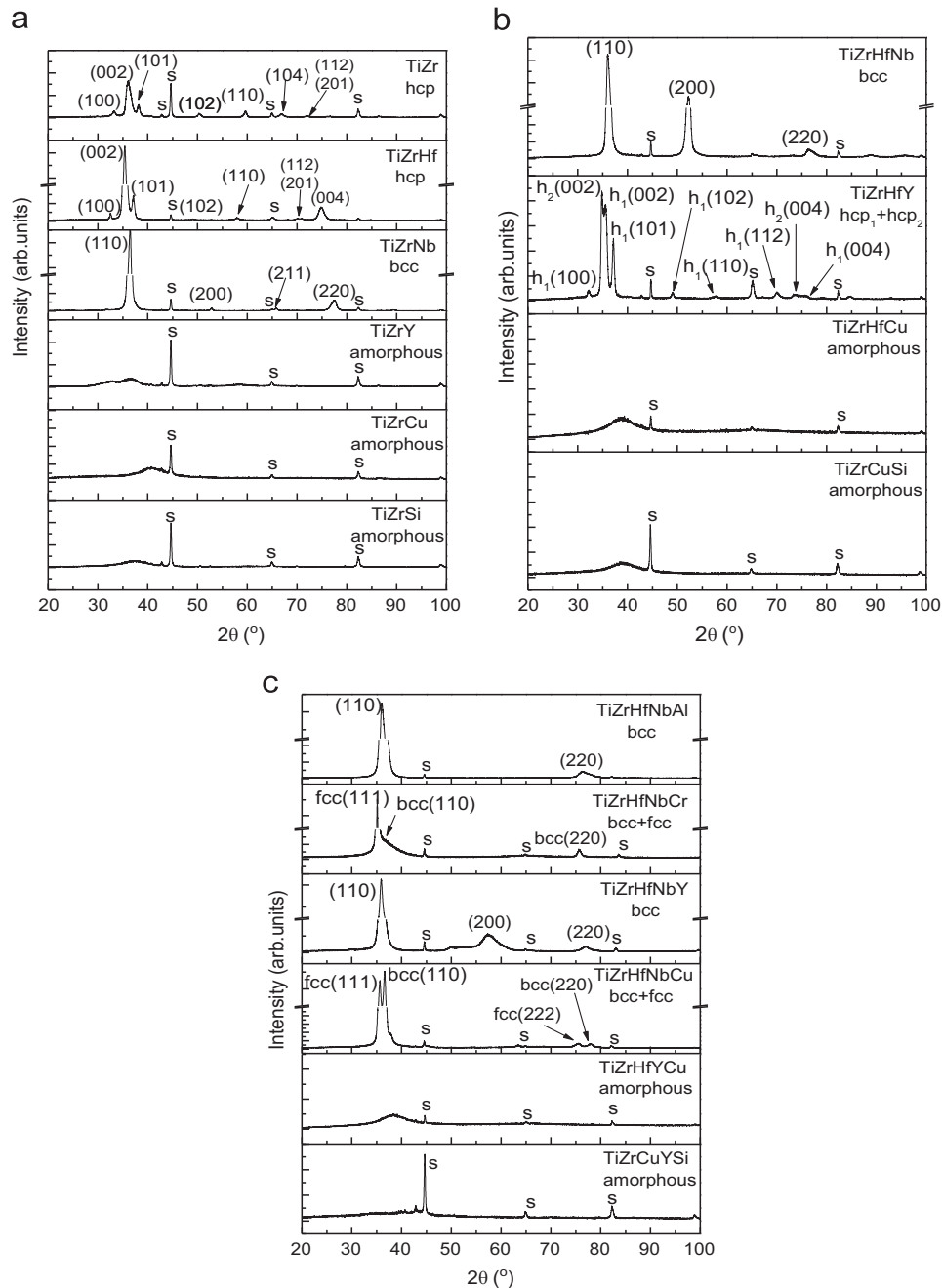


Fig. 1. XRD spectra of the deposited films: (a) binary and ternary and (b) quaternary and (c) quinternary metallic films.

In the case of quinternary films, the bcc TiZrNbHf system keeps its bcc structure at Al or Y incorporation, while the Cr and Cu addition determined the formation of a mixture of phases (bcc + fcc). The other quinternary films (TiZrYCuNb and TiZrYCuSi) were found to be amorphous, most probably due to Cu and Si presence.

The above results can be summarized as follows:

- Whatever the type and number of components, no intermetallic compounds formed.
- The type of crystalline structure of TiZr-based MPE films depended on the specific elements incorporated in the

binary to quaternary films. As in the case of ternary compounds, it was found that Hf was acting as hcp stabilizer for the quaternary films. Yttrium addition determined the amorphisation of the ternary films, while in quaternary films was acting as hcp stabilizer. Nb and Al served as bcc stabilizers, and Cu as fcc stabilizer. Similar results were reported in the case of other HEAs, for which Al was considered to stabilize a bcc structure, while fcc phase was stabilized by Cu, Co or Ni [14,29].

- Concerning the crystallinity, Nb and Hf addition facilitated the formation of solid solution phases, while Cu and Si, were acting as amorphous phase forming elements.

Table 1
Crystalline structure, lattice parameters and crystallite size $\langle d \rangle$ of the deposited films.

No.	Film	Crystalline structure	Lattice parameters (nm)	$\langle d \rangle$ (nm)
1	TiZr	hcp	$\langle a \rangle = 0.3111$ $\langle c \rangle = 0.4887$	14.2
2	TiZrHf	hcp	$\langle a \rangle = 0.3175$ $\langle c \rangle = 0.5069$	17.0
3	TiZrNb	hcp	$\langle a \rangle = 0.3473$	17.2
4	TiZrY	Amorphous	–	–
5	TiZrCu	Amorphous	–	–
6	TiZrSi	Amorphous	–	–
7	TiZrHfNb	bcc	$\langle a \rangle = 0.3528$	12.0
8	TiZrHfY	hcp ₁	$\langle a \rangle = 0.3214$ $\langle c \rangle = 0.5148$	19.2
		hcp ₂	$\langle a \rangle = 0.3182$ $\langle c \rangle = 0.5033$	9.9
		Amorphous	–	–
9	TiZrHfCu	Amorphous	–	–
10	TiZrCuSi	Amorphous	–	–
11	TiZrHfNbAl	bcc	$\langle a \rangle = 0.3531$	10.6
12	TiZrHfNbCr	bcc	$\langle a \rangle = 0.3463$	2.3
		fcc	$\langle a \rangle = 0.4424$	25.5
13	TiZrHfNbY	bcc	$\langle a \rangle = 0.3536$	12.6
		hcp	$\langle a \rangle = 0.2231$ $\langle c \rangle = 0.3207$	3.1
		bcc	$\langle a \rangle = 0.3467$ $\langle a \rangle = 0.4360$	17.0 18.5
14	TiZrHfNbCu	bcc	$\langle a \rangle = 0.3467$ $\langle a \rangle = 0.4360$	17.0 18.5
15	TiZrHfYCu	Amorphous	–	–
16	TiZrCuYSi	Amorphous	–	–

Since, as already shown, the films exhibited large differences in their structures (from amorphous to crystalline), in the following we will analyze the factors responsible for this behavior.

4. Discussion

To understand the factors that mainly control the film crystallinity, we considered the existing models concerning the processes and phenomena which can affect the stability of phases in multicomponent alloys. The models comprise the formation rules for solid solution phases in multicomponent alloys [15,18,20], and also for amorphous phases in bulk metallic glasses [24,33]. To accommodate with the experimental findings, there were derived some empirical rules, which were generally described in terms of atomic-size effects of the constituent atoms, and also of thermodynamical functions, being numerically interpreted to give the variation ranges of significant parameters for formation of a certain phase type. For calculating the thermodynamical functions, the regular solution model was commonly considered by different authors (e.g. [33] and the references therein), and will be also used in the present study.

The main factors which can control the phase formation and stability in multicomponent alloys are the difference in atomic radii, the enthalpy of mixing, the mixing entropy and the Gibbs

free energy of mixing of the solid-solutions and amorphous phases, and the electronegativity difference, as described below:

- Difference in atomic radii, described by the parameter δ [14,18,34]:

$$\delta = 100 \sqrt{\sum_{i=1}^n c_i \left(1 - \frac{r_i}{\bar{r}}\right)^2} \quad (1)$$

where n is the number of constituents, c_i is the atomic percentage of the I component, r_i is the atomic radius and $\bar{r} = \sum_{i=1}^n c_i r_i$ is the average atomic radius.

- Enthalpy of mixing (formation) of the solid solution phase ΔH^{ss} , which is considered to characterize the chemical compatibility between the constituents and, according to the regular solution model and Miedema's approach, can be written as [35,33] follows:

$$\Delta H^{ss} = \Delta H^{ch} + \Delta H^{el} \quad (2)$$

where ΔH^{ch} and ΔH^{el} are the chemical and elastic contributions to enthalpy, respectively.

For a multicomponent system, if only binary interactions are considered, ΔH^{ch} and ΔH^{el} are given by the following equation:

$$\Delta H^{ch} = \sum_{i,j} c_i c_j \Omega_{ij} \quad (3)$$

where $\Omega_{ij} (= 4\Delta H_{AB}^{mix})$ is the regular solution interaction parameter and ΔH_{AB}^{mix} is the mixing enthalpy for binary solid solutions (ΔH_{AB}^{mix} values can be found in Ref. [36])

$$\Delta H^{el} = \sum_{i=1, i \neq j}^n c_i c_j (c_i h_{i \text{ in } j}^{el} + c_j h_{j \text{ in } i}^{el}) \quad (4)$$

where $\Delta h_{i \text{ in } j}^{el}$ can be calculated using [37,33]:

$$\Delta h_{i \text{ in } j}^{el} = \frac{2\mu_j (V_i - V_j)^2}{V_j (3 + 4\mu_j k_i)} \quad (5)$$

Here, μ_j is the shear modulus of the solvent, V_i and V_j are the molar volumes of the solute and the solvent, respectively and K_i is the compressibility of the solute, and can be found, e.g., in [38].

- Enthalpy of mixing of the solid solution amorphous phase ΔH^{am} , calculated by the following equation [33,39]:

$$\Delta H^{am} = \Delta H^{ch} + \sum_{i=1}^n c_i H_i^a \quad (6)$$

where H_i^a is the enthalpy of amorphous pure metals, which can be expressed as follows [33,35]:

$$H_i^a = \alpha T_{m,i} \quad (7)$$

with $T_{m,i}$ – the melting point of the i th component and $\alpha = 3.5 \text{ J mol}^{-1} \text{ K}^{-1}$

- Mixing entropy of the solid solution phase ΔS^{ss} is defined as follows [24]:

$$\Delta S^{ss} = \Delta S^{conf} + \Delta S^\delta \quad (8)$$

where $\Delta S^{conf} = -R \sum_{i=1}^n (c_i \ln c_i)$, with R is Boltzmann's constant, is the ideal configurational entropy, and ΔS^δ is the mismatch term resulting from different atomic size values, and can be calculated as function of the atomic radii, composition and packing fraction [24,40,41].

- Mixing entropy of the amorphous phase ΔS^{am} is defined as follows [35,42]:

$$\Delta S^{am} = \Delta S^{conf} + \Delta S^{dis} \quad (9)$$

The entropy change ΔS^{dis} is determined by the specific disordering character of the amorphous phase, being estimated as $\Delta S^{dis} = 3.5 \text{ J mol}^{-1} \text{ K}^{-1}$.

- Gibbs free energy of mixing of the solid solution ΔG^{ss} (expressing the change of Gibbs free energy for the system transition from the elemental to the crystalline mixed states):

$$\Delta G^{ss} = \Delta H^{ss} - T_d \Delta S^{ss} \quad (10)$$

where T_d – the deposition temperature of the film, was chosen as a significant temperature – dependent parameter of the thin film formation process.

- Gibbs free energy of mixing of the amorphous phase ΔG^{am} .

$$\Delta G^{am} = \Delta H^{am} - T_d \Delta S^{am} \quad (11)$$

- The electronegativity difference $\Delta \chi$ is determined by the following equation [18]:

$$\Delta \chi = \sqrt{\sum_{i=1}^n c_i (\chi_i - \bar{\chi})^2} \quad (12)$$

with $\bar{\chi} = \sum_{i=1}^n c_i \chi_i$ where χ_i is the Pauling electronegativity for the i th component.

It should be noticed that in this work we preferred to follow the simplified schemes used in the Refs. [15,18,24,33], based on the enthalpies of formation of binary compounds estimated with Miedema's model, in which the multiple interaction parameters are neglected. This model was used for estimating the formation enthalpy of the ternary, quaternary and quinary alloy systems mainly because the input data needed in calculation do not require additional experimental data, which may be unavailable. There are known some extrapolation methods, proposed in order to extend Miedema's model to compounds with more components. For example, the ternary atomic interactions between the constituents were also considered [43] or, in the model elaborated by Goncalves et al., the crystallographic positions of the atoms were taken into account [44], while the scheme of Ouyang et al. included the asymmetry of thermodynamic properties of the constitutive binary systems [45]. However, these theories are not only difficult to be used in calculations for quaternary and quinary alloys, but also need additional information which in some cases is not reliable, and the final results are still depending on empirical parameters.

The above described parameters, calculated for the films investigated in this work, are listed in Table 2. A careful examination of data in the table indicates the main parameters dictating the formation of an either crystalline or amorphous phase.

When focusing on differences in atomic radii (δ parameter), it can be seen that solid solution phases form for $\delta < 8.6$, while amorphous phases for $\delta > 8.6$. We would mention that $\delta = 8.6$ appears to be a threshold value, for which it is formed either a solid solution (TiZrHfNbY) or an amorphous phase (TiZrHfCu). This is an expected result, as it is in line with one of the requirements from classical Hume-Rothery rules for

Table 2

Atomic size difference δ , chemical contribution of the enthalpy of mixing ΔH^{ch} , enthalpy of mixing of the solid solution ΔH^{ss} , enthalpy of mixing of the amorphous phase ΔH^{am} , configurational entropy ΔS^{conf} , Gibbs free energy of mixing of the solid solution ΔG^{ss} , Gibbs free energy of mixing of the amorphous phase ΔG^{am} , and electronegativity difference $\Delta \chi$. Gray rows are indicating the amorphous films.

Film	δ	ΔH^{ch} ($\times 10^3 \text{ J mol}^{-1}$)	ΔH^{ss} ($\times 10^3 \text{ J mol}^{-1}$)	ΔH^{am} ($\times 10^3 \text{ J mol}^{-1}$)	ΔS^{conf} ($\text{J K}^{-1} \text{ mol}^{-1}$)	ΔS^{ss} ($\text{J K}^{-1} \text{ mol}^{-1}$)	ΔG^{ss} ($\times 10^3 \text{ J mol}^{-1}$)	ΔG^{am} ($\times 10^3 \text{ J mol}^{-1}$)	$\Delta \chi$
TiZr	4.6	0.0	4.2	7.1	5.76	6.15	0.7	1.8	0.105
TiZrHf	4.0	0.0	2.4	7.6	9.13	9.42	-3.0	0.4	0.107
TiZrNb	5.0	2.7	4.7	10.6	9.13	9.61	-0.8	3.4	0.116
TiZrY	8.6	10.7	19.4	17.5	9.13	10.49	13.4	10.3	0.133
TiZrCu	9.2	-14.2	-3.7	-7.9	9.13	10.65	-9.8	-15.1	0.235
TiZrSi	13.4	-66.7	-64.8	-60.0	9.13	12.16	-71.8	-67.2	0.235
TiZrHfNb	4.9	2.5	4.4	10.6	12.64	13.08	-3.1	1.4	0.130
TiZrHfY	7.6	8.8	14	16.0	12.64	13.72	6.1	6.8	0.118
TiZrHfCu	8.7	-12.3	-4.3	-5.3	12.64	13.96	-12.3	-14.6	0.239
TiZrCuSi	12.5	-50.3	-43.8	-44.0	12.64	15.42	-52.6	-53.3	0.244
TiZrHfNbAl	5.0	-19.4	-17.9	-12.2	13.38	13.84	-25.8	-21.9	0.134
TiZrHfNbCr	8.6	-4.0	2.3	4.0	13.38	14.69	-6.1	-5.7	0.145
TiZrHfNbY	8.3	12.0	16.3	19.7	13.38	14.69	7.9	10.1	0.146
TiZrHfNbCu	7.9	-5.8	-0.8	1.7	13.38	14.50	-9.1	-8.0	0.217
TiZrHfYCu	11.2	-5.8	3.4	1.0	13.38	15.66	-5.6	-8.7	0.245
TiZrCuYSi	15.8	-43.5	-34.5	-37.3	13.38	17.69	-44.6	-47.0	0.282

binary alloys: to form a solid solution, the constituent elements must possess similar atomic size. Otherwise, a significant lattice distortion occurs, accompanied by the corresponding strain energy increase, leading to separation or segregation of different elements, or to amorphisation. It should be noted that for bulk high-entropy alloys, the solid solution were also found to form, starting from relative low values of δ : $\delta \leq 6$ [18], $\delta \leq 6.6$ [19] or $\delta \leq 8.5$ [15].

If we look to the thermodynamic functions specific for the phase formation in multicomponent alloy systems, it is to mention that the chemical enthalpy ΔH^{ch} was considered by many authors as one of the main factors that control the phase formation (e.g. [14,15,18,20]). This enthalpy, that is a measure of the chemical compatibility between the components, was also taken into account by one of the Hume-Rothery rules, according to which a solid solution tends to form when the constituent elements have small chemical enthalpy differences. As pointed out by Yang and Zhang in a recent work [20], in the case of HEAs, a large value of ΔH^{ch} (either negative or positive) hinders the formation of a solid solution. For this type of alloys, it was reported that for forming solid solution phases, the variation domain of ΔH^{ch} should be -15×10^3 – 5×10^3 J mol⁻¹ [18], or -22×10^3 – 7×10^3 J mol⁻¹ [15], or -5×10^3 – 5×10^3 J mol⁻¹ [14]. In the case of our films, if we consider only the value of ΔH^{ch} , it would be difficult to discriminate between the formation of either a solid solution or an amorphous phase. Though, in general, the solid solutions formed for low ΔH^{ch} values (e.g. TiZrHf, TiZrHfNb, TiZrHfNbCr), in line with the results for HEAs, there exist some exceptions: crystalline TiZrHfY or TiZrHfYNb films with relative high ΔH^{ch} values (8.8×10^3 J mol⁻¹ and 12.0×10^3 J mol⁻¹, respectively) and amorphous TiZrHfYCu with low ΔH^{ch} (-5.8×10^3 J mol⁻¹).

The results concerning the effects of chemical enthalpy ΔH^{ch} on phase formation in multicomponent metallic films can be examined in Fig. 2. As discussed before, it is apparent that,

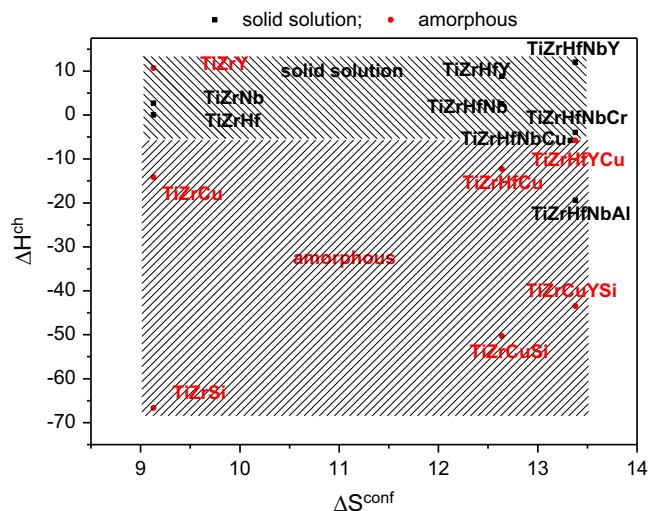


Fig. 2. The relation between ΔS^{conf} and ΔH^{ch} for solid solution or amorphous phase formation in the investigated films.

in general, amorphous phases tend to form at more negative values of (ΔH^{ch}).

On the other side, it is worth to compare the mixing enthalpy values of the solid solution phase ΔH^{ss} with those of mixing enthalpy of amorphous phase ΔH^{am} . According to Miedema's approach, an amorphous phase forms when its formation enthalpy is smaller than that of the solid solution [46]. Following this model, Basu et al. determined the composition range for forming an amorphous phase in (Zr, Ti, Hf)–(Cu, Ni) binary and ternary alloys [33], with a good agreement between the calculated and experimental results. It can be seen that the above mentioned criterion works well for all the investigated films, as the condition $\Delta H^{am} < \Delta H^{ss}$ is fulfilled for the amorphous films (TiZrY, TiZrCu, TiZrSi, TiZrHfCu, TiZrCuSi, TiZrHfYCu and TiZrCuYSi), while for the crystalline films (TiZr, TiZrHf, TiZrNb, TiZrHfNb, TiZrHfY, TiZrHfNbAl, TiZrHfNbCr, TiZrHfNbY and TiZrHfNbCu), $\Delta H^{am} > \Delta H^{ss}$. Following only this criterion, the TiZrSi film is an exception since ΔH^{ss} (TiZrSi) = -64.8×10^3 J mol⁻¹ is lower than ΔH^{am} (TiZrSi) = -60.0×10^3 J mol⁻¹. However one may observe that for TiZrSi the atomic size difference is very large ($\delta = 14.4$) and also the chemical enthalpy is highly negative ΔH^{ch} (TiZrSi) = -66.7×10^3 J mol⁻¹, so that the amorphous phase formation is explained by the fulfilment of other criteria for amorphous phase formation.

To predict the equilibrium state of an alloy, the effect of entropy change between the elemental and mixed state was widely discussed, especially concerning solid solution phase formation in high entropy alloys [1,7,18,20]. It was judged that the high mixing entropy specific to HEAs is responsible for the preferential formation of solid solutions instead of intermetallic compounds. A high mixing entropy reduces the tendency of ordering and segregation of the constituents and thus restrains the formation of intermetallics or other ordered phases [7,18,20].

As for the formation of amorphous phases, Guo and Liu [14], analyzing literature data concerning phase stability in HEAs, found that a high value of mixing entropy (between 13.38 and 14.89 J K⁻¹ mol⁻¹, corresponding to quinary and senary compounds, respectively) favors amorphous phase formation. We should underline that in this analysis, as well as in other similar studies [18,20], only the configurational entropy ΔS^{conf} was calculated. For our ternary to quinary films, it can be seen that the increase in configurational entropy from 9.13 to 13.38 J K⁻¹ mol⁻¹ did not affect film crystallinity: both solid solutions and amorphous phases were formed for $\Delta S^{conf} = 9.13$ J K⁻¹ mol⁻¹ and for $\Delta S^{conf} = 13.38$ J K⁻¹ mol⁻¹. In other words, the solely increase in the number of components did not favor the films' crystallinity. An adequate thermodynamic analysis of phase formation in multicomponent systems has to take into account the Gibbs free energy of mixing ΔG^{mix} , which is the thermodynamic potential commonly used for predicting the equilibrium state in a system. The standard procedure is as follows (e.g. [12,16,36,47]). The phases possibly to be formed are evaluated and compared: the phase with lower ΔG^{mix} value will form preferentially. For the

films investigated in this work, free energies were calculated for both solid solution and amorphous phase, using the formulae (10) and (11), respectively, in which, beside the chemical enthalpy ΔH^{ch} and the configurational entropy ΔS^{conf} , additional significant terms were taken into account for a more precise determination of the free energies.

Data in Table 2 show that amorphous phase forms when $\Delta G^{am} < \Delta G^{ss}$, similarly to mixing enthalpies relations. It can also be seen that the most films with amorphous structures fall in the region with more negative ΔG values. It should be noticed that the increase of the number of constituent elements did not favor the formation of certain structure type. Therefore, it can be concluded that the formation of solid solution or amorphous phase in MPE metallic films is mainly determined by the characteristics of the components and not by their number (reflected in the value of the configurational entropy). This finding is in line with the results reported by Guo et al. [15] and Zhang et al. [18], who also considered that the configurational entropy is not a decisive factor in determining the crystalline structure of a high entropy alloy.

As for the electronegativity difference $\Delta\chi$, this parameter, similarly to ΔH^{ch} , characterizes the chemical affinity between the constituent elements in a multicomponent system. Data in Table 2 show that for the amorphous films (except for TiZrY), the $\Delta\chi$ value is relatively high, exceeding ~ 0.230 , while the crystalline films possess a much lower $\Delta\chi$ value, in the range 0.105–0.146. Therefore, as a first degree approximation, the electronegativity difference could be also taken as a reliable parameter for predicting the crystallinity of a multicomponent metallic film.

It is important to note that the deposition conditions of the investigated films are also determining the energetic conditions under which the film structures were developed. A change of these parameters is expected to affect the phase formation. Therefore, further studies are under development in order to analyze the influence of the relevant deposition conditions (substrate temperature, ion bombardment of the substrate) upon the phase composition and crystalline structure, and also to correlate the film structure and morphology to its mechanical, anti-corrosive and tribological characteristics.

5. Conclusions

TiZr-based multi-principal-element metallic thin films with 3–5 components were deposited by co-sputtering of metallic targets. Other elements (Hf, Nb, Al, Cu, Cr, Y and Si) were combined in the deposited films, so that for the deposition temperature of 300 °C, no intermetallic compounds were detected by X-ray diffraction. The analysis of the thermodynamics and atomic size factors which can control the phase formation has been conducted, and the following main results, validated by the experimental approach, are reported as follows:

1. The relationship between the Gibbs free energy of mixing of solid solution (ΔG^{SS}) and amorphous (ΔG^{am}) phases, and atomic size difference (δ) are proposed as criteria for predicting phase formation in multi-principal-element metallic films.
2. Amorphous phases were formed when the following conditions were simultaneously satisfied: $\Delta G^{am} < \Delta G^{SS}$ and $\delta > 8.6$.
3. Certain elements can be used to tune the microstructure of the films: the hcp structure is stabilized by either Hf or Y, bcc by Nb or Al, fcc by Cu, while Si facilitates amorphous phase formation.

Acknowledgments

This work was supported by Grant of the Romanian National Authority for Scientific Research, CNCS-UEFISCDI, Romania with the Project number PN-II-ID-PCE-2011-3-1016.

References

- [1] J.H. Westbrook, *Intermetallic Compounds: Principles and Practice*, Wiley, New York, 1995.
- [2] J.R., Davis (Ed.), *Metals Handbook*, tenth ed., ASM International, Metals Park, OH, 1990, vol. 1.
- [3] A.L. Greer, *Nature* 366 (1993) 303–304.
- [4] B. Cantor, I.T.H. Chang, P. Knight, A.J.B. Vincent, *Mater. Sci. Eng. A* 375–377 (2004) 213–218.
- [5] J.H. Westbrook, R.L. Fleischer, John Wiley & Sons, New York, 2000.
- [6] J.W. Yeh, S.K. Chen, S.J. Lin, J.Y. Gan, T.S. Chin, T.T. Shun, C. H. Tsau, S.Y. Chang, *Adv. Eng. Mater.* 6 (2004) 299–303.
- [7] J.W. Yeh, *Ann. Chim. Sci. Mater.* 31 (2006) 633–648.
- [8] C.P. Lee, C.C. Chang, Y.Y. Chen, J.W. Yeh, H.C. Shih, *Corros. Sci.* 50 (2008) 2053–2060.
- [9] K.C. Hsieh, C.F. Yu, W.T. Hsieh, W.R. Chiang, J.S. Ku, J.H. Lai, C. P. Tu, C.C. Yang, *J. Alloys Compd.* 483 (2009) 209–212.
- [10] Y.L. Chen, Y.H. Hu, C.W. Tsai, C.A. Hsieh, S.W. Kao, J.W. Yeh, T. S. Chin, S.K. Chen, *J. Alloys Compd.* 477 (2009) 696–705.
- [11] K. Zhang, Z. Fu, J. Zhang, W. Wang, H. Wang, Y. Wang, Q. Zhang, *Mater. Sci. Forum* 620–622 (2009) 383–386.
- [12] A. Li, X. Zhang, *Acta Metall. Sin.* 22 (2009) 219–224.
- [13] S. Singh, N. Wanderka, B.S. Murty, U. Glatzel, J. Banhart, *Acta Mater.* 59 (2011) 182–190.
- [14] S. Guo, C. Ng, J. Lu, C.T. Liu, *J. Appl. Phys.* 109 (2011) 103505–103510.
- [15] S. Guo, C.T. Liu, *Prog. Nat. Sci.* 21 (2011) 433–446.
- [16] Y. Zhang, G. Chen, C. Gan, *J. ASTM Int.* 7 (2010) 1–8.
- [17] Y. Zhang, *Mater. Sci. Forum* 654–656 (2010) 1058–1061.
- [18] Y. Zhang, Y.J. Zhou, J.P. Lin, G.L. Chen, P.K. Liaw, *Adv. Eng. Mater.* 10 (2008) 534–538.
- [19] Y. Zhang, W. Jie Peng, *Procedia Eng.* 27 (2012) 1169–1178.
- [20] X. Yang, Y. Zhang, *Mater. Chem. Phys.* 132 (2012) 233–238.
- [21] Y.J. Zhou, Y. Zhang, F.J. Wang, G.L. Chen, *Appl. Phys. Lett.* 90 (2007) 181904–181907.
- [22] S. Wang, H. Ye, *Adv. Mater. Res.* 338 (2011) 380–383.
- [23] X.Q. Gao, K. Zhao, H.B. Ke, D.W. Ding, W.H. Wang, H.Y. Bai, *J. Non-cryst. Solids* 357 (2011) 3557–3560.
- [24] A. Takeuchi, A. Inoue, *Mater. Sci. Eng. A* 304–306 (2001) 446–451.
- [25] R.W. Cahn, P. Hassen, North Holland, Amsterdam, 1996, vol. 1.
- [26] K. Cheng, C. Lai, S. Lin, J. Yeh, *Ann. Chim. Sci. Mater.* 31 (2006) 723–736.
- [27] C.H. Lai, S.J. Lin, J.W. Yeh, S.Y. Chang, *Surf. Coat. Technol.* 201 (2006) 3275–3280.
- [28] P.K. Huang, J.W. Yeh, *Surf. Coat. Technol.* 203 (2009) 1891–1896.

- [29] V. Dolique, A.L. Thomann, P. Brault, Y. Tessier, P. Gillon, *Surf. Coat. Technol.* 204 (2010) 1989–1992.
- [30] C.H. Lin, J.G. Duh, *Surf. Coat. Technol.* 203 (2008) 558–561.
- [31] J.E. Krzanowski, *Surf. Coat. Technol.* 188–189 (2004) 376–383.
- [32] B.T. Wang, W.D. Li, P. Zhang, *J. Nucl. Mater.* 420 (2012) 501–507.
- [33] J. Basu, B.S. Murty, S. Ranganathan, *J. Alloys Compd.* 465 (2008) 163–172.
- [34] S. Fang, X. Xiao, L. Xia, W. Li, Y. Dong, *J. Non-cryst. Solids* 321 (2003) 120–125.
- [35] G.J. Van der Kolk, A.R. Miedema, A.K. Niessen, *J. Less Common Met.* 145 (1988) 1–17.
- [36] A. Takeuchi, A. Inoue, *Mater. Trans.* 46 (2005) 2817–2829.
- [37] S. Simozar, J.A. Alonso, *Phys. Status Solidi A* 81 (1984) 55–61.
- [38] E.A. Brandes, *Smithells Metals Reference Book*, sixth ed., Butterworth, London, 1983.
- [39] Z.J. Zhang, H.Y. Bai, Q.Y. Qin, T. Yang, K. Tao, B.x. Lin, *J. Appl. Phys.* 73 (1993) 1702–1710.
- [40] G.A. Mansoori, N.F. Carnahan, K.E. Starling, T.W. Leland, *J. Chem. Phys.* 54 (1971) 1523–1526.
- [41] I.H. Umar, I. Yokoyama, W.H. Young, *Philos. Mag.* 34 (1976) 535–548.
- [42] T. Mousavi, M.H. Abbasi, F. Karimzadeh, *Mater. Lett.* 63 (2009) 786–788.
- [43] S.L. Lin, Z.R. Nie, H. Huang, C.Y. Zhan, Z.B. Xing, W. Wang, *Trans. Nonferrous Met. Soc. China* 20 (2010) 682–687.
- [44] A.P. Gonçalves, M. Almeida, *Phys. B Condens. Matter* 228 (1996) 289–294.
- [45] Y. Ouyang, X. Zhong, H. Shi, Y. Du, Y. He, *Mater. Trans.* 47 (2006) 388–391.
- [46] A.R. Miedema, *Philips Tech. Rev.* 36 (1976) 217–231.
- [47] S. Sabooni, F. Karimzadeh, M.H. Abbasi, *Bull. Mater. Sci.* 35 (2012) 439–447.